

# Thermodynamically self-consistent liquid state theories for systems with bounded potentials

Bianca M. Mladek<sup>a)</sup>

Center for Computational Materials Science, Vienna University of Technology, A-1060 Vienna, Austria  
and Institut für Theoretische Physik, TU Wien, Wiedner Hauptstraße 8-10, A-1040 Wien, Austria  
and Institut für Experimentalphysik, Universität Wien, Strudlhofgasse 4, A-1090 Wien, Austria

Gerhard Kahl

Center for Computational Materials Science, Vienna University of Technology, A-1060 Vienna, Austria  
and Institut für Theoretische Physik, TU Wien, Wiedner Hauptstraße 8-10, A-1040 Wien, Austria

Martin Neumann

Institut für Experimentalphysik, Universität Wien, Strudlhofgasse 4, A-1090 Wien, Austria

(Received 16 September 2005; accepted 22 December 2005; published online 10 February 2006)

The mean spherical approximation (MSA) can be solved semianalytically for the Gaussian core model (GCM) and yields exactly the same expressions for the energy and the virial equations. Taking advantage of this semianalytical framework, we apply the concept of the self-consistent Ornstein-Zernike approximation (SCOZA) to the GCM: a state-dependent function  $K$  is introduced in the MSA closure relation which is determined to enforce thermodynamic consistency between the compressibility route and either the energy or virial route. Utilizing standard thermodynamic relations this leads to two differential equations for the function  $K$  that have to be solved numerically. Generalizing our concept we propose an integrodifferential-equation-based formulation of the SCOZA which, although requiring a fully numerical solution, has the advantage that it is no longer restricted to the availability of an analytic solution for a particular system. Rather it can be used for an arbitrary potential and even in combination with other closure relations, such as a modification of the hypernetted chain approximation. © 2006 American Institute of Physics.

[DOI: 10.1063/1.2167646]

## I. INTRODUCTION

It is meanwhile well-known and widely documented that conventional integral equation theories—such as the Percus-Yevick (PY), the hypernetted chain (HNC), or the mean spherical (MSA) approximation—are thermodynamically inconsistent, which means that the various thermodynamic routes to calculate the dimensionless equation of state lead to significantly different results.<sup>1,2</sup> Over the past decades considerable effort has been devoted to the formulation of thermodynamically self-consistent liquid state theories, which, in turn, have led to an improved description of the structural and thermodynamic properties of liquids with harshly repulsive potentials. In the first generation of these concepts, such as the Rogers-Young (RY),<sup>3</sup> the modified hypernetted chain (MHNC),<sup>4</sup> or the Zerah-Hansen approach,<sup>5</sup> simple functions were introduced in the respective closure relations to the Ornstein-Zernike (OZ) equation which use a pointwise adjustable but not explicitly state-dependent parameter to interpolate between the conventional closures. Since self-consistency was enforced for each state point independent of the neighboring ones, we shall call this approach *locally self-consistent*. The concepts of the second generation of the self-consistent liquid state theories were based on more sophisticated ideas: the self-consistent Ornstein-Zernike ap-

proximation (SCOZA)<sup>6</sup> introduced an explicitly state-dependent function in the MSA closure relation to the OZ equation in order to enforce thermodynamic self-consistency between different thermodynamic routes; the hierarchical reference theory (HRT),<sup>7</sup> on the other hand, successfully merged ideas of microscopic liquid state theory and renormalization group concepts. In both these advanced liquid state approaches thermodynamic consistency was enforced in the *entire* space of system parameters, which we shall call *global self-consistency*.

In recent years, increasing effort has been devoted to investigations of the structural and thermodynamic properties of soft matter systems.<sup>8</sup> The interactions in such systems either diverge weakly or even remain finite (“bounded”) at short distances, i.e., when particles overlap. These potentials are commonly referred to as soft potentials. Initially, they were investigated by means of conventional<sup>8</sup> and, more recently, by means of locally self-consistent integral-equation theories.<sup>9,10</sup> However, the advanced liquid state theories mentioned above have not been generalized to systems with soft potentials so far. The HRT concept, for instance, relies on the known properties of a suitable reference system. While for systems with strongly repulsive interactions the hard-core (HC) liquid represents an obvious and very successful choice, no such reference system can be identified for liquids with soft potentials. We therefore have to rule out HRT, at least for the time being.

<sup>a)</sup>Electronic mail: mladek@tph.tuwien.ac.at

On the other hand, applications of the SCOZA concept<sup>6</sup> to liquid systems were up to now restricted to those cases where the respective interactions can be expressed as a combination of HC potentials with an adjacent linear combination of Yukawa tails [so-called hard-core Yukawa (HCY) systems].<sup>11</sup> This restriction can be traced back to the fact that the rather elaborate SCOZA formalism<sup>6</sup> is intricately linked to the availability of the analytic solution of the MSA for such a system.<sup>12</sup> From this point of view the obvious counterpart of HCY systems in soft matter is the Gaussian core model (GCM).<sup>13</sup> For this system the pair potential is given by

$$\Phi(r) = \varepsilon \exp[-(r/\sigma)^2], \quad (1)$$

where  $\varepsilon$  is an energy parameter and  $\sigma$  is a length parameter.

Within the framework of the MSA (in the case of soft potentials sometimes also termed random phase approximation), the structural and thermodynamic properties of the GCM can to a large extent be expressed semianalytically.<sup>9,14</sup> In this contribution we extend the SCOZA formalism to the GCM.

The GCM can be interpreted as a simple model to describe soft matter. It has been pointed out that, for example, the effective (coarse-grained) interaction between two isolated nonintersecting polymer chains or dendritic macromolecules can, to a very good approximation, be represented by the GCM potential.<sup>15,16</sup> In our effort to apply the concept of global thermodynamic self-consistency to systems with soft potentials, the GCM represents *the* ideal candidate. Based on the analytic expressions given by the MSA for the energy and the virial route of the GCM, it is possible to derive a partial differential equation (PDE) for the state-dependent function introduced in the closure relation of the SCOZA which relates both density and temperature derivatives. Two alternative ways to enforce thermodynamic consistency can be formulated by using the virial and the compressibility routes. On the one hand, this leads to an ordinary differential equation (ODE) that can be solved for each isothermal line independently. On the other hand, we propose an integrodifferential equation (IDE) based formulation of the SCOZA, which has to be solved fully numerically. This latter approach has the advantage that it can be used for an arbitrary (soft) potential and in combination with closure relations other than the MSA, such as, e.g., a HNC-based SCOZA ansatz; thus, it is no longer restricted to systems where semi-analytic solutions of liquid state theories are known.

The rest of the paper is organized as follows: in Sec. II we revisit the MSA for the GCM, providing thus the basis for the (semi)analytic formulation of the SCOZA. In Sec. III we present the ideas of SCOZA and derive the two differential equations and the IDE that impose self-consistency and in Sec. IV we present details about the numerical solution strategies. Section V is devoted to a detailed discussion of the SCOZA results and a comparison with Monte Carlo (MC) simulation data. Finally, in Sec. VI we summarize and draw our conclusions.

## II. MSA

For the GCM, semianalytic expressions for the static and thermodynamic properties can be derived within the MSA.<sup>9,14</sup> Here we add a few details that have not been documented yet.

The MSA closure relation to the Ornstein-Zernike (OZ) equation,

$$h(r) = c(r) + \varrho \int d\mathbf{r}' h(|\mathbf{r} - \mathbf{r}'|) c(r'), \quad (2)$$

where  $h(r)$  and  $c(r)$  are the total and the direct correlation functions and  $\varrho$  is the number density of the system, was originally proposed for systems for which the pair potential consists of a HC interaction with diameter  $\sigma$  plus a tail that can take different functional forms.<sup>1</sup> For such potentials, the MSA consists of an ansatz for  $c(r)$ ,

$$c(r) = -\beta\Phi(r) \quad \text{for } r > \sigma, \quad (3)$$

where  $\beta = (k_B T)^{-1}$ ,  $T$  is the temperature, and  $k_B$  Boltzmann's constant, along with the so-called core condition that expresses the impenetrability of the particles,

$$g(r) = 0 \quad \text{for } r < \sigma. \quad (4)$$

Here,  $g(r) = h(r) + 1$  is the radial distribution function (RDF).

As soft potentials lack a hard core, Eq. (4) cannot be applied anymore and the MSA reduces to

$$c(r) = -\beta\Phi(r) \quad \text{for all } r. \quad (5)$$

For the specific case of the GCM, where  $\Phi(r)$  is a simple Gaussian, this immediately leads to an analytic expression for the static structure factor,  $S(q)$ ,

$$S(q) = [1 - \varrho \hat{c}(q)]^{-1} = \frac{1}{1 + \alpha \exp[-(q^2 \sigma^2/4)]}, \quad (6)$$

where the hat denotes a Fourier transform,  $q$  is the wave vector, and  $\alpha = \pi^{3/2} \varrho \sigma^3 \beta \varepsilon$ . For the RDF we find

$$g(r) = 1 - \frac{\alpha}{\varrho} \frac{1}{8\pi^3} \int d\mathbf{q} e^{-i\mathbf{q}\mathbf{r}} \frac{1}{e^{q^2 \sigma^2/4} + \alpha}; \quad (7)$$

in particular,

$$g(0) = 1 + \frac{\beta\varepsilon}{\alpha} \text{Li}_{3/2}(-\alpha). \quad (8)$$

Here,  $\text{Li}_n(x)$  is the polylogarithm of order  $n$  which is discussed in detail in the Appendix.

Furthermore, the thermodynamic properties of the GCM can be calculated semianalytically using one of the usual three thermodynamic routes.<sup>1</sup> The results for the dimensionless equation of state,  $\beta P/\varrho$ , where  $P$  is the pressure, obtained via the compressibility route (C),

$$\left(\frac{\beta P}{\varrho}\right)^C = 1 + \frac{1}{2}\alpha, \quad (9)$$

and the virial route (V),

$$\left(\frac{\beta P}{\rho}\right)^V = 1 + \frac{1}{2}\alpha - \beta\varepsilon\aleph(\alpha), \quad (10)$$

where

$$\aleph(\alpha) = \frac{1}{2\alpha}[\text{Li}_{3/2}(-\alpha) - \text{Li}_{1/2}(-\alpha)], \quad (11)$$

have already been reported in Refs. 9 and 14.

The energy route ( $E$ ) has not been considered in the literature so far. To obtain  $(\beta P/\rho)^E$  we first calculate the excess (over ideal gas) internal energy per particle,  $U^{\text{ex}}/N$ ,

$$\frac{\beta U^{\text{ex}}}{N} = 2\pi\beta\rho \int_0^\infty dr\Phi(r)g(r)r^2 = \frac{\alpha}{2} - \frac{\beta\varepsilon}{2\alpha}[\alpha + \text{Li}_{3/2}(-\alpha)], \quad (12)$$

from which we obtain the excess free energy per particle,  $F^{\text{ex}}/N$ ,

$$\frac{\beta F^{\text{ex}}}{N} = \int_0^\beta d\beta' \frac{U^{\text{ex}}(\beta', \rho)}{N} = \frac{\alpha}{2} - \frac{\beta\varepsilon}{2\alpha}[\alpha + \text{Li}_{3/2}(-\alpha)], \quad (13)$$

and, finally, the equation of state,

$$\left(\frac{\beta P}{\rho}\right)^E = 1 + \rho \frac{\partial}{\partial \rho} \left(\frac{\beta F^{\text{ex}}}{N}\right) = 1 + \frac{1}{2}\alpha - \beta\varepsilon\aleph(\alpha). \quad (14)$$

Thus we find that virial (10) and energy routes (14) lead *exactly* to the same expressions for the dimensionless equation of state.

### III. SCOZA

The original formulation of the SCOZA for HC systems<sup>6</sup> is based on the MSA. It enforces the RDF to vanish inside the core and for distances larger than the core diameter sets the direct correlation function proportional to the potential; the proportionality factor contains a state-dependent function that imposes thermodynamic consistency. Following the same scheme used to generalize the MSA to soft potentials (see Sec. II), we modify the original SCOZA ansatz,

$$c(r) = \beta K_i(\rho, \beta)\Phi(r) \quad \text{for all } r; \quad i = \text{EC or VC}, \quad (15)$$

where  $K_i(\rho, \beta)$  are as yet undetermined, state-dependent functions and the subscripts EC and VC specify which routes are used to enforce thermodynamic self-consistency. For those formulas common to both cases, the subscript  $i$  will be used. As the MSA is recovered for  $K_i(\rho, \beta) \equiv -1$ , the present formulation of the SCOZA takes advantage of the availability of the semianalytic solution of the MSA for the GCM presented in the preceding subsection.

Thus, closed expressions can be derived for the thermodynamic properties within the SCOZA. To simplify the notation we introduce a function  $\tilde{\alpha}_i(\rho, \beta) = \pi^{3/2}\rho\sigma^3\beta\varepsilon K_i(\rho, \beta) = \alpha K_i(\rho, \beta)$ , which is explicitly state dependent, but for simplicity we suppress the arguments of  $\tilde{\alpha}_i$  in the following.

According to the compressibility route the density derivative of the equation of state is given by

$$(\chi_{\text{red}}^C)^{-1} = (\rho k_B T \chi_T^C)^{-1} = 1 - \rho \hat{c}(0) = 1 - \tilde{\alpha}_i, \quad (16)$$

where  $\chi_T^C$  is the isothermal compressibility and the reduced isothermal compressibility  $\chi_{\text{red}}^C$  is the zero wave-vector value of the structure factor  $S(q)$ .

Furthermore, following the virial route one finds the following expression for the dimensionless equation of state:

$$\begin{aligned} \left(\frac{\beta P}{\rho}\right)^V &= 1 - \frac{2\pi}{3}\rho \int_0^\infty dr r^3 \frac{d\beta\Phi(r)}{dr} g(r) \\ &= 1 + \frac{1}{2}\alpha - \frac{\beta\varepsilon}{2\tilde{\alpha}_i}[\text{Li}_{5/2}(\tilde{\alpha}_i) - \text{Li}_{3/2}(\tilde{\alpha}_i)]. \end{aligned} \quad (17)$$

Finally, according to the energy route the dimensionless excess energy per particle is given by

$$\frac{\beta U^{\text{ex}}}{N} = \frac{1}{2}\alpha + \frac{\beta\varepsilon}{2\tilde{\alpha}_i}[\text{Li}_{3/2}(\tilde{\alpha}_i) - \tilde{\alpha}_i]. \quad (18)$$

The thermodynamic inconsistency can be removed either via the energy/compressibility or via the virial/compressibility route; both possibilities will be considered in the following subsections.

#### A. Energy and compressibility route

To enforce thermodynamic consistency between the energy and compressibility route we utilize the variant of the SCOZA formalism proposed in Refs. 17 and 18 which brought along a breakthrough of this concept for systems with repulsive potentials. Historically seen, this represents the conventional approach to SCOZA. It is based on replacing the differential equation for  $K_{\text{EC}}(\rho, \beta)$  by one for the excess energy density  $u = U^{\text{ex}}/V$ . To this end, we consider the following thermodynamic relation (see, e.g., Ref. 19):

$$\frac{\partial}{\partial \beta} \left( \frac{1}{\chi_{\text{red}}^E} \right) = \rho \frac{\partial^2 u}{\partial \rho^2}. \quad (19)$$

Expressing at constant density  $\chi_{\text{red}}^E$  as a function of  $u$ , the left-hand side can be rewritten as

$$\frac{\partial}{\partial \beta} \left( \frac{1}{\chi_{\text{red}}^E(u)} \right) = \frac{\partial}{\partial u} \left( \frac{1}{\chi_{\text{red}}^E(u)} \right) \frac{\partial u}{\partial \beta}, \quad (20)$$

so that finally Eq. (19) becomes

$$\frac{\partial u}{\partial \beta} = \left[ \frac{\partial}{\partial u} \left( \frac{1}{\chi_{\text{red}}^E(u)} \right) \right]^{-1} \rho \frac{\partial^2 u}{\partial \rho^2}. \quad (21)$$

This relation contains derivatives with respect to both  $\rho$  and  $\beta$  and is a PDE of the diffusion type. However, the diffusivity,  $D(\rho, \beta) = [(\partial/\partial u)\rho(1/\chi_{\text{red}}^E(u))]^{-1}$ , is state dependent<sup>20</sup> and turns out to be negative.  $\chi_{\text{red}}^E(u)$  is now identified with the expression obtained by the compressibility route (16),

$$[\chi_{\text{red}}^C(u)]^{-1} = 1 - \tilde{\alpha}_{\text{EC}}, \quad (22)$$

where  $K_{\text{EC}}(u)$  is determined by inverting the result of the energy route,

$$u = \frac{\varrho}{\beta} \left\{ \frac{1}{2} \alpha + \frac{\beta \varepsilon}{2 \tilde{\alpha}_{\text{EC}}} [\text{Li}_{3/2}(\tilde{\alpha}_{\text{EC}}) - \tilde{\alpha}_{\text{EC}}] \right\}. \quad (23)$$

## B. Virial and compressibility route

As an alternative to the approach presented in the preceding subsection, we can calculate the compressibility via the *virial* route,  $\chi_T^V$ , which is achieved by differentiating Eq. (17) with respect to  $\varrho$ ,

$$\frac{\partial K_{\text{VC}}(\varrho, \beta)}{\partial \varrho} = \frac{K_{\text{VC}}(\varrho, \beta) \{ 2\pi^3 \beta \varepsilon \varrho^2 \sigma^6 K_{\text{VC}}(\varrho, \beta) [K_{\text{VC}}(\varrho, \beta) + 1] - [\text{Li}_{3/2}(\tilde{\alpha}_{\text{VC}}) - \text{Li}_{1/2}(\tilde{\alpha}_{\text{VC}})] \}}{\varrho [2\text{Li}_{3/2}(\tilde{\alpha}_{\text{VC}}) - \text{Li}_{5/2}(\tilde{\alpha}_{\text{VC}}) - \text{Li}_{1/2}(\tilde{\alpha}_{\text{VC}})]}. \quad (25)$$

Note that this ODE can be solved for each isothermal line separately.

Analyzing the ODE, we note that the right-hand side (RHS) of Eq. (25) contains two singularities. Obviously the denominator vanishes for  $\varrho \rightarrow 0$ , but expanding numerator and denominator around  $\varrho=0$ , we find that

$$K_{\text{VC}}(\varrho=0; \beta) = -\frac{4\sqrt{2}}{4\sqrt{2} + \beta \varepsilon}. \quad (26)$$

Furthermore, the denominator also vanishes at  $\tilde{\alpha}_{\text{VC}} = \tilde{\alpha}_{\text{VC},0} \approx -7.7982$ . This, however, turns out to be a removable singularity which can be treated by appropriate means (see Sec. IV B).

## C. Integrodifferential equation approach

So far, in deducing both the SCOZA-ODE (25) and PDE (21), we have taken advantage of the availability of the semi-analytic framework provided by the MSA for the properties of the GCM. Unfortunately, this represents a rather singular exception. In order to eliminate the restrictions resulting from this fact one may ask whether the SCOZA concept may be formulated for the *general* case, i.e., when a semianalytic solution to the MSA is not at hand. This is indeed possible as we show in the following: let us assume a SCOZA-type closure relation, i.e.,

$$c(r) = \beta \bar{K} \Phi(r) \quad \text{for all } r. \quad (27)$$

Once  $\bar{K}$  is specified, this leads in combination with the OZ equation directly to the radial distribution function  $g(r) = g(r; \varrho, \beta; \bar{K})$ , which is thus also a function of  $\bar{K}$ . If we assume  $\bar{K}$  to be explicitly state dependent, i.e.,  $\bar{K} = \bar{K}(\varrho, \beta)$ , the compressibility as determined by the virial route, i.e., differentiating the standard virial equation of state, is

$$\begin{aligned} \left( \frac{\partial \beta P}{\partial \varrho} \right)^V &= 1 + \alpha - \frac{1}{2\sigma^3 \pi^{3/2} K_{\text{VC}}(\varrho, \beta)^2} \\ &\times \left\{ \frac{K_{\text{VC}}(\varrho, \beta)}{\varrho} [\text{Li}_{3/2}(\tilde{\alpha}_{\text{VC}}) - \text{Li}_{1/2}(\tilde{\alpha}_{\text{VC}})] \right. \\ &+ \frac{\partial K_{\text{VC}}(\varrho, \beta)}{\partial \varrho} [2\text{Li}_{3/2}(\tilde{\alpha}_{\text{VC}}) - \text{Li}_{5/2}(\tilde{\alpha}_{\text{VC}}) \\ &\left. - \text{Li}_{1/2}(\tilde{\alpha}_{\text{VC}})] \right\}. \quad (24) \end{aligned}$$

Equating this result with the compressibility as obtained via the compressibility route (16) leads to the following ODE for the unknown function  $K_{\text{VC}}(\varrho, \beta)$ :

$$\begin{aligned} [\varrho k_B T \chi_T^V]^{-1} &= 1 - \frac{4\pi}{3} \varrho \int_0^\infty dr r^3 \frac{d\beta \Phi(r)}{dr} g(r; \varrho, \beta; \bar{K}) \\ &- \frac{2\pi}{3} \varrho^2 \int_0^\infty dr r^3 \frac{d\beta \Phi(r)}{dr} \frac{\partial g(r; \varrho, \beta; \bar{K})}{\partial \varrho} \\ &- \frac{2\pi}{3} \varrho^2 \frac{\partial \bar{K}}{\partial \varrho} \int_0^\infty dr r^3 \frac{d\beta \Phi(r)}{dr} \frac{\partial g(r; \varrho, \beta; \bar{K})}{\partial \bar{K}}. \quad (28) \end{aligned}$$

Thermodynamic self-consistency between the virial and the compressibility route is now enforced by choosing the mixing parameter  $\bar{K}$  such that  $\chi_T^C$  is equal to  $\chi_T^V$ , i.e., by finding at fixed temperature  $T$  a root of the function,

$$f(\bar{K}) = \chi_T^C - \chi_T^V. \quad (29)$$

Here, derivatives with respect to  $\varrho$  and  $\bar{K}$  have to be calculated numerically (see below).

It was exactly this idea that was realized in previous applications of parametrized closure relations such as RY,<sup>3</sup> HMSA,<sup>5</sup> or MHNC.<sup>4</sup> There, however, consistency was then achieved only *locally*, i.e., considering each state point in isolation and neglecting thus the density dependence of  $\bar{K}$ . This corresponds to setting  $\partial \bar{K} / \partial \varrho = 0$  and dropping the last term in Eq. (28). In the present approach, in contrast, since we consider  $\bar{K}$  to be explicitly state dependent, this term is retained. Thus, the consistency criterion involves not only isolated state points but also via the density derivative nearby state points; therefore we have chosen to call the criterion a *global* one. The quantitative difference between the local and the global approaches will be discussed below.

## D. HNC-based SCOZA

The above approach to thermodynamic consistency represents an IDE-based reformulation of the SCOZA; it is not only entirely independent of the semianalytic solution provided by the MSA for the GCM and thus becomes completely *general* in the sense that in this formulation self-consistency can now be enforced for systems with *arbitrary* (soft) potentials and in combination with other, parametrized closure relations.

To demonstrate the power of this idea we introduce a HNC-based SCOZA (for clarity we will refer to the SCOZA approaches introduced above as “MSA-based SCOZA”). This particular choice is motivated by the fact that the HNC has been found to work very well for the GCM and other soft potentials.<sup>9,14</sup> For the closure relation of our HNC-based SCOZA we propose

$$g(r) = \exp[\beta \bar{K}_{\text{HNC}}(\varrho, \beta) \Phi(r) + h(r) - c(r)], \quad (30)$$

where the unknown, state-dependent function  $\bar{K}_{\text{HNC}}(\varrho, \beta)$  is determined such as to make the right-hand side (RHS) of the consistency requirement (29), i.e., the equality between the compressibility and the virial route, vanish. Numerically, this is achieved by solving Eq. (28), where  $g(r; \varrho, \beta; \bar{K}_{\text{HNC}})$  is now obtained from the solution of the OZ equation along with the closure relation (30).

## IV. NUMERICAL SOLUTION OF THE SCOZA AND COMPUTER SIMULATIONS

### A. PDE approach

From the numerical point of view, solving the diffusion-type SCOZA-PDE (21) is a delicate task, as we have to face the problem of a state-dependent diffusivity  $D(\varrho, \beta)$ . Since this quantity is even negative, not only the solution to the PDE but any numerical error incurred in obtaining it may be expected to grow exponentially. Among other things, small errors made in the formulation of the boundary conditions and the inversion of the highly nonlinear relation (23) to determine  $D(\varrho, \beta)$  will eventually get dominant. Together, these difficulties make it practically impossible to reliably solve this PDE. Reversing the direction in which the PDE is solved would represent a solution to this problem, unfortunately, the initial condition for  $\beta\varepsilon = \infty$  is not known.

### B. ODE approach

The SCOZA-ODE (25), on the other hand, has the attractive feature that it can be solved for each isothermal line independently and represents thus a fast route to determine  $K_{\text{VC}}(\varrho, \beta)$ . We have used an implicit fourth-order Runge-Kutta algorithm<sup>21</sup> to solve this ODE numerically. This works generally very well except for those state points where the expression in the square brackets of the denominator of the RHS of Eq. (25) vanishes. A closer analysis shows that this singularity at  $\tilde{\alpha}_{\text{VC}} = \tilde{\alpha}_{\text{VC},0}$  is removable, since both numerator and denominator vanish simultaneously. In fact, splitting the density range in two regions, depending on whether  $\tilde{\alpha}_{\text{VC}}$  is smaller or larger than  $\tilde{\alpha}_{\text{VC},0}$ , and integrating the ODE “forward” [starting at  $\varrho=0$  with initial value (26)] in the former

and “backward” (from a sufficiently high density so that  $K_{\text{VC}} = -1$ ) in the latter, we were able to smoothly join the partial solutions at  $\tilde{\alpha}_{\text{VC}} = \tilde{\alpha}_{\text{VC},0}$  and thus to obtain  $K_{\text{VC}}(\varrho, \beta)$  over the entire density range. We point out that reliable solutions of this ODE can only be obtained if an efficient and accurate evaluation of the polylogarithm is guaranteed (see Appendix).

Alternatively, we have also solved this ODE with MATHEMATICA using a Livermore solver for ordinary differential equations with automatic method switching (LSODA).<sup>22</sup> The polylogarithms encountered in the RHS of Eq. (25) are evaluated in MATHEMATICA with high accuracy (for details see Ref. 22). Although the differential-equation-solver package is not able to deal properly with the removable singularity noted above and breaks down for  $\tilde{\alpha}_{\text{VC}} \sim \tilde{\alpha}_{\text{VC},0}$ , outside this small range, MATHEMATICA provides quasiexact reference data for the function  $K_{\text{VC}}(\varrho, \beta)$ .

### C. IDE approach

The IDE-based formulation of the SCOZA, i.e., Eq. (29) along with (28), has been solved iteratively using both the MSA-based (27) and the HNC-based closure (30). We introduce a density grid (with spacing  $\Delta\varrho$ ) and assume a starting value  $\bar{K} = -1$ . We solve the OZ equation with the appropriate closure relation using standard integral-equation solver algorithms for a given state point (i.e., we fix  $\varrho$  and  $\beta$ ) and the neighboring density values (i.e., for  $\varrho \pm \Delta\varrho$ ). Thus, the derivatives in the RHS of Eq. (28) can be calculated numerically. Due to the appearance of the derivative  $\partial\bar{K}/\partial\varrho$ , Eq. (28) has to be solved iteratively and leads then to  $\bar{K}(\varrho, \beta)$  for the *entire* density range considered. As a consequence of the iterative and purely numerical character of the solution strategy, this approach is more time consuming than the solution of the ODE (25).

### D. Monte Carlo simulations

To test the reliability of our integral equation results we have generated reference data for the GCM by means of standard MC simulations in the canonical ensemble. For each thermodynamic state considered, we started from a random configuration of  $N=1000$  particles. The system was at first allowed to equilibrate for 10 000 sweeps, where a sweep consists of  $N$  trial moves, i.e., on average each particle has been subjected to a trial move once. After that, we have carried out production runs of another 150-300 000 sweeps to calculate the desired ensemble averages.

## V. RESULTS

As a solution to the PDE approach could not be obtained, we concentrate our discussions on the results of the ODE and the IDE, which represent equivalent approaches and thus are expected to lead to the same result. We start by specifying the range in  $(\varrho, \beta)$  space where the MSA and the SCOZA provide unphysical results, i.e., where  $g(r)$  is negative (see Fig. 1). While this failure of the MSA was briefly addressed in Ref. 14, we think that a more *quantitative*

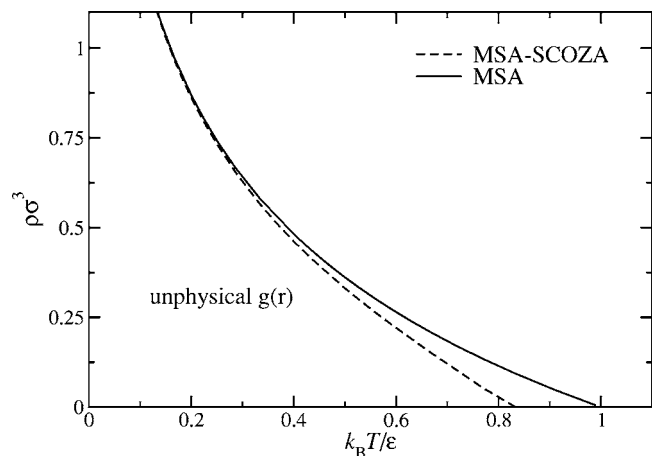


FIG. 1. Region in the density-temperature space, where the MSA and the MSA-based SCOZA provide unphysical results, i.e., the RDF  $g(r)$  attains negative values.

analysis is in order, since similar problems might be encountered in applications of the MSA (and of related concepts) to other systems with soft potentials. In fact, also for the SCOZA unphysical results can be obtained for certain system parameter combinations. For the MSA the limits of this range of unphysical behaviour are easily determined via Eq. (8), and for the SCOZA they are found from the equivalent, generalized expression (i.e., replacing  $\alpha$  by  $\tilde{\alpha}_{VC}$ ). Results are shown in Fig. 1, indicating that at low temperatures the MSA and the SCOZA both become unphysical if the density is reduced below some threshold density  $\varrho = \varrho(\beta)$ . It is interesting to note that similar problems of unphysical solutions and thus restricted applicability have also been reported for other self-consistent schemes, such as the RY or the zero-separation concepts, in combination with the GCM.<sup>9</sup>

Detailed numerical investigations have shown that—as expected—the solution to the ODE provides the same results as the one from the IDE. Thus, we present the state-dependent function  $K_{VC}(\varrho, \beta) \equiv \bar{K}(\varrho, \beta)$  as obtained from

the solution of the SCOZA-PDE (25) [and the IDE approach to the MSA-based SCOZA closure (27), respectively] in Fig. 2 in a representative part of the parameter space. Bearing in mind that the MSA is recovered for  $\bar{K}(\varrho, \beta) \equiv -1$ , we observe that this function differs substantially from this value at low densities (with a pronounced temperature dependence), thus indicating those regions where the MSA is thermodynamically inconsistent. At high densities we confirm earlier results reported in Refs. 9 and 14, which have stated that in this regime the MSA becomes exact and thus self-consistent. While in Ref. 14 this conclusion was based on an analysis of the large density behavior of the function  $\aleph$  as defined in Eq. (11), our argumentation follows directly from a visual inspection of the function  $\bar{K}(\varrho, \beta)$ .

Taking into consideration that the virial and the energy routes coincide within the MSA, an open question that remains is whether this also holds for SCOZA. To this end, we take  $K_{VC}(\varrho, \beta)$  as obtained from the ODE (25) and insert it into Eq. (21). We find that this relation is numerically fulfilled very accurately. This can be seen as an indication that  $K_{VC}(\varrho, \beta)$  imposes thermodynamic consistency even between all three thermodynamic routes. However, this cannot be proved analytically.

For the HNC-based SCOZA, the corresponding function,  $\bar{K}_{HNC}(\varrho, \beta)$  is shown in Fig. 3. Taking the deviation of this function from  $-1$  as a measure of the thermodynamic inconsistency of the simple HNC approach (similar to the case of the MSA), we observe that the HNC is to a large degree self-consistent. It is only at small densities and low temperatures that  $\bar{K}_{HNC}(\varrho, \beta)$  slightly deviates from  $-1$ . This large degree of thermodynamic self-consistency of the HNC for systems with bounded potentials was already observed for selected state points in Refs. 9 and 14, but was never demonstrated on a quantitative level for a wider range of system parameters.

We conclude our discussion of the thermodynamic self-consistency of the MSA-based and the HNC-based SCOZA

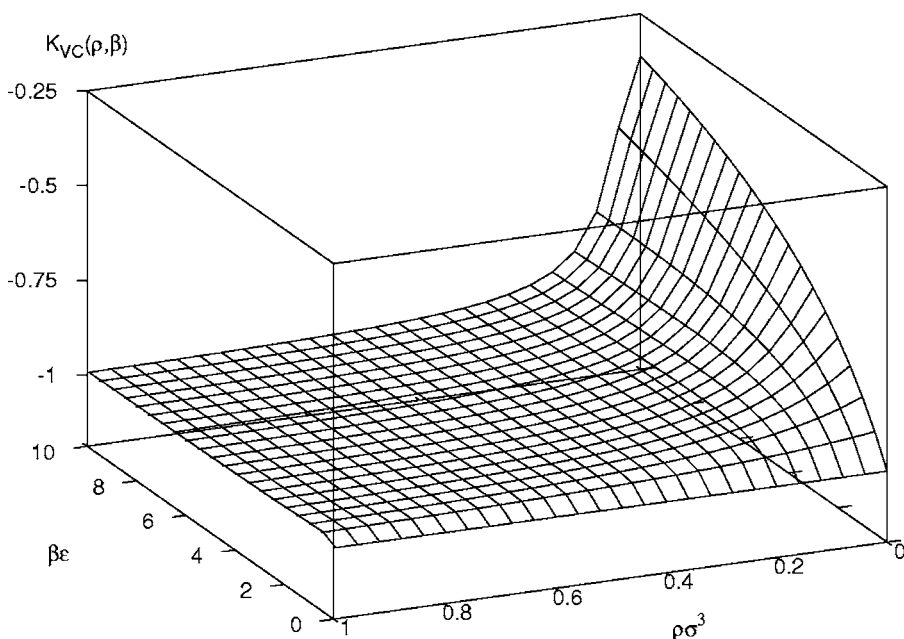


FIG. 2.  $K_{VC}(\varrho, \beta) \equiv \bar{K}(\varrho, \beta)$  as obtained from the solution of the SCOZA-PDE (25) [and the IDE approach to the MSA-based SCOZA closure (27), respectively] over a representative range of  $\varrho\sigma^3$  and  $\beta\epsilon$ . Note that  $\beta\epsilon$  is the inverse reduced temperature, i.e., high values of  $\beta\epsilon$  correspond to low temperatures.

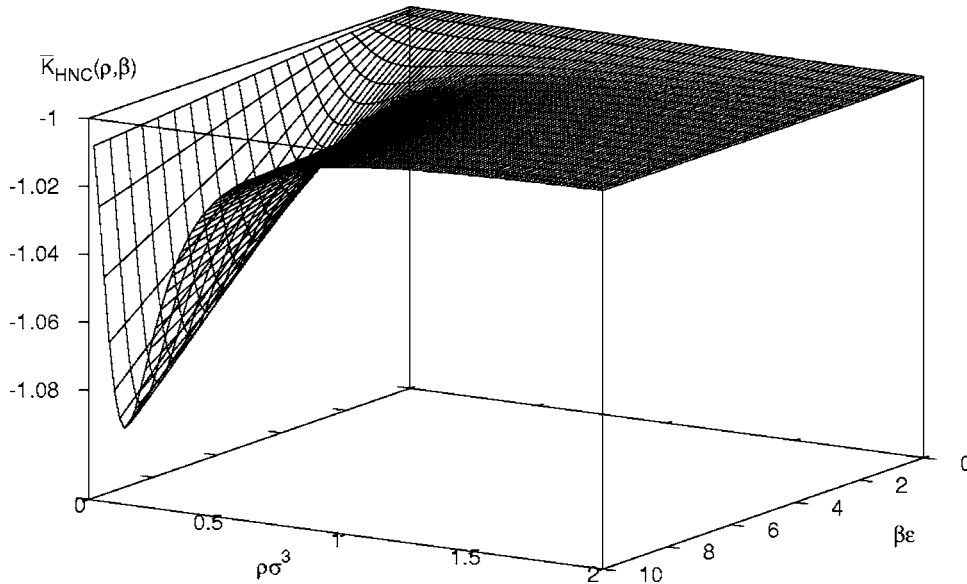


FIG. 3.  $\bar{K}_{\text{HNC}}(\rho, \beta)$  as obtained from the solution of the IDE approach to the HNC-based SCOZA closure (30) over a representative range of  $\rho\sigma^3$  and  $\beta\epsilon$ . Note that, in an effort to enhance the visibility of the data, the viewpoint is now different from the one in Fig. 2.

concepts by a direct comparison between local and global self-consistency, as defined in Sec. III C. Let  $\bar{K}_g(\rho, \beta)$  denote the explicitly state-dependent function  $\bar{K}(\rho, \beta)$ , as introduced to enforce thermodynamic self-consistency in the IDE formulation of the (MSA- or HNC-based) SCOZA (see Sec. III C); thus, the subscript *g* stands for *global* self-consistency. On the other hand, if the last term in Eq. (28) is neglected thermodynamic self-consistency is only enforced for a single, isolated state point and in this case we denote the function by  $\bar{K}_l(\rho, \beta)$  (*local* self-consistency). In Fig. 4 we show the relative difference between these functions for the MSA-based SCOZA and we observe that it amounts to a few percent only for small densities, even down to intermediate temperatures. Figure 5 shows the same function for the HNC-based SCOZA. Here, the differences become noticeable only at small densities and low temperatures. Thus, over

a large parameter range local consistency is in both cases already a good substitute for global consistency.

We now turn to the structural properties of the GCM by comparing the RDFs for two different thermodynamic states. In Fig. 6, we have chosen a state point close to the boundary where the MSA-based SCOZA becomes unphysical (see Fig. 1). We observe that compared to the MC reference data, the MSA-based SCOZA does bring along a slight improvement over the MSA. On the other hand, the results provided by the HNC and the HNC-based SCOZA both reproduce the MC data perfectly. Figure 7 shows the RDF for the GCM at a low temperature and low density. Here, we are in the regime where both the MSA and the MSA-based SCOZA provide unphysical results. We see that while the conventional HNC results already reproduce the MC data rather well, the HNC-based SCOZA leads to a perfect agreement with the simula-

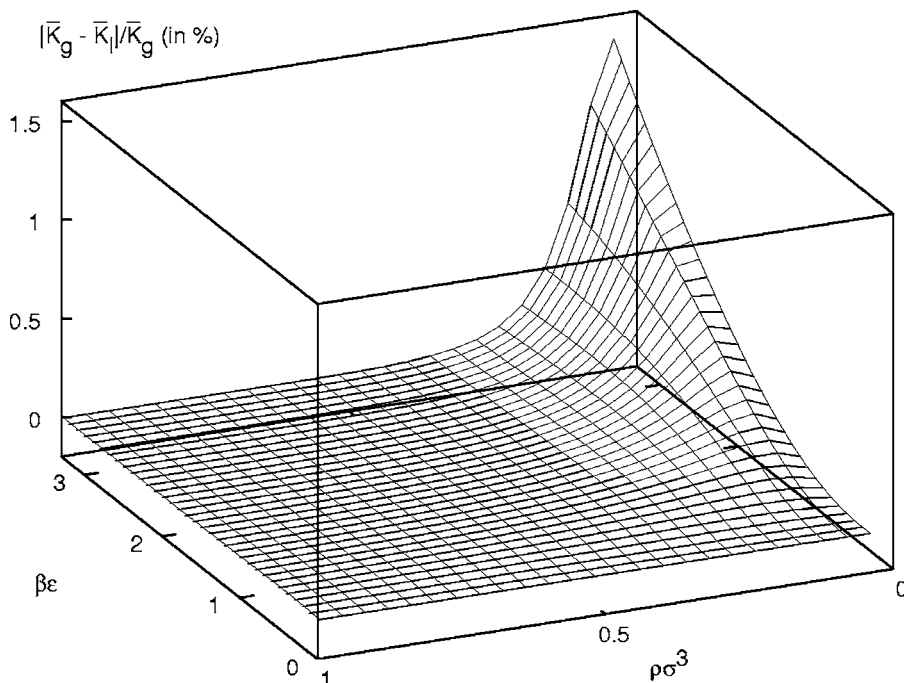


FIG. 4. Relative difference between the functions  $\bar{K}_g$  and  $\bar{K}_l$  (as defined in the text) over a representative range of  $\rho\sigma^3$  and  $\beta\epsilon$ .

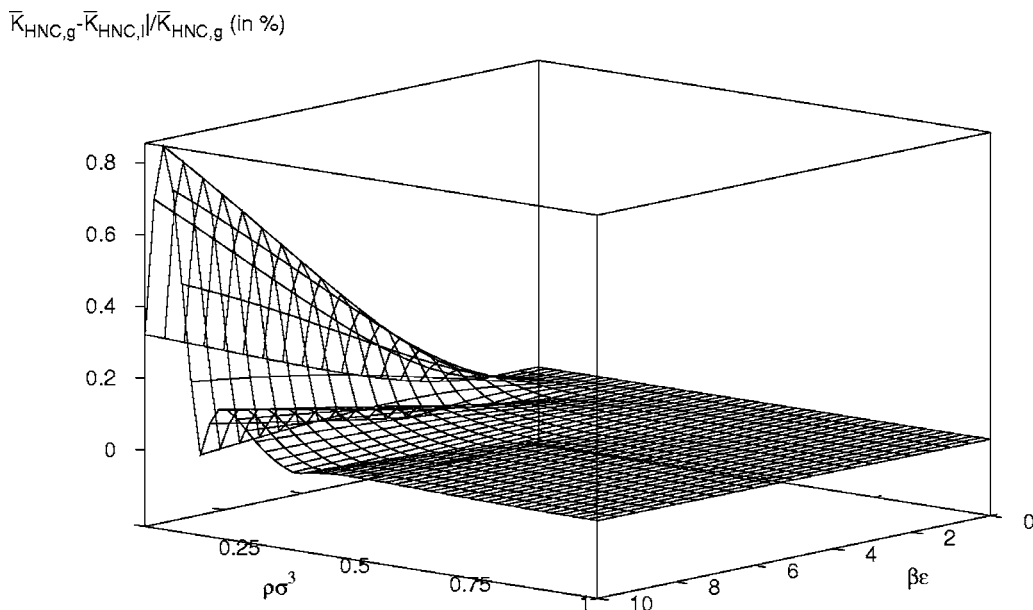


FIG. 5. Relative difference between the functions  $\bar{K}_{\text{HNC},g}$  and  $\bar{K}_{\text{HNC},l}$  (as defined in the text) over a representative range of  $\beta\epsilon$  and  $\rho\sigma^3$ . Note that, in an effort to enhance the visibility of the data, the viewpoint is now different from the one in Fig. 4.

tions. We conclude, that although the MSA-based SCOZA for the GCM does not bring along the same improvement for the structural properties as documented for HCY systems, the concept of self-consistency by itself proves to be of great value when used with a closure better adapted to bounded potentials, i.e., a HNC-based closure.

Finally, we conclude this section by examining thermodynamic properties and present the results for the dimensionless equation of state,  $\beta P/\rho$ , for two different temperatures, i.e.,  $k_B T/\epsilon=10$  (see Fig. 8) and  $k_B T/\epsilon=0.1$  (see Figs. 9 and 10). For  $k_B T/\epsilon=10$ , we find that the SCOZA results coincide with high accuracy with the MC data. For  $k_B T/\epsilon=0.1$  we observe (Fig. 9) that the MSA-based SCOZA provides data that are obviously very close to those obtained by simulations, while the HNC-based SCOZA data fit them perfectly. A more thorough comparison, including this time also other liquid state theories, such as the MSA, the Percus-Yevick (PY), or the HNC approximations,<sup>1</sup> is displayed on an en-

larged scale in Fig. 10. We observe that in addition also the virial route of the PY and of the HNC (as expected<sup>9,14</sup>) nicely reproduce the MC data; however, while the SCOZA is self-consistent, this is not the case for the conventional closure relations HNC and PY: their respective compressibility data sometimes differ distinctively from their virial and/or energy results.

Thus we can conclude that the general concept of the SCOZA *does* bring along an improvement over conventional liquid state theories for a thermodynamically consistent description of the properties of the GCM, in particular, if used in combination with a modification of the HNC closure. It is especially remarkable that also the structural properties are enhanced, even though the SCOZA scheme only enforces self-consistency for the thermodynamic properties.

## VI. CONCLUSION

Motivated by the success of the SCOZA to describe the properties of HC systems, we have made first steps to extend

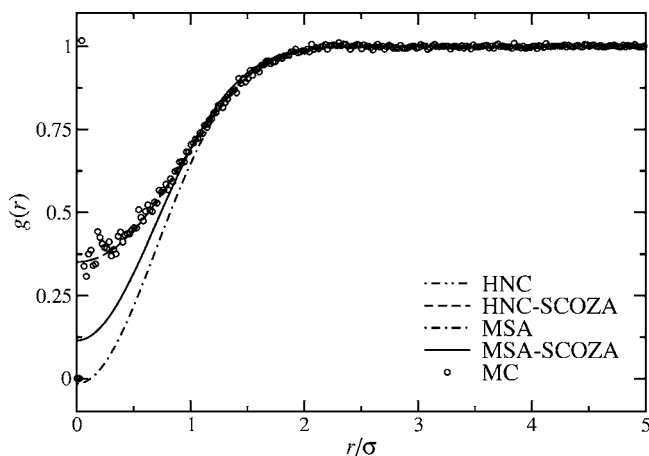


FIG. 6. RDF  $g(r)$  for the GCM for  $\beta\epsilon=1.1$  and  $\rho\sigma^3=0.04$ . Note that the HNC and the HNC-based SCOZA curves coincide within line thickness.

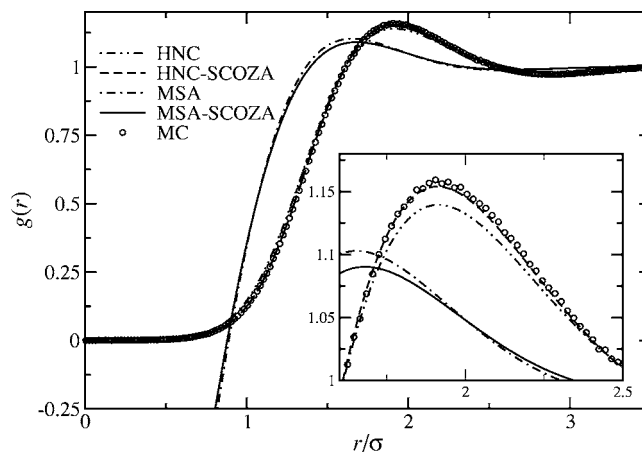


FIG. 7. RDF  $g(r)$  for the GCM for  $\beta\epsilon=10$  and  $\rho\sigma^3=0.14$ .

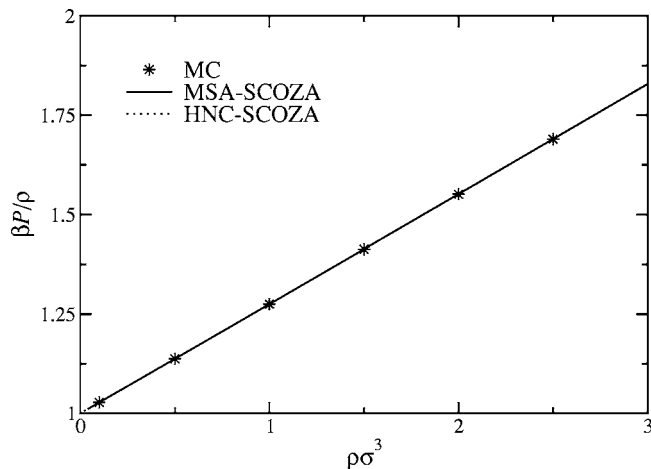


FIG. 8.  $\beta P/\rho$  as a function of  $\rho\sigma^3$  for the GCM for  $k_B T/\varepsilon=10$ . The results of the SCOZA and the HNC-based SCOZA coincide. Both SCOZA approaches provide physical data for the RDF [i.e.,  $g(r)>0$ ] over the entire density range.

this concept to systems with soft potentials. The fact that the MSA can be solved semianalytically for the GCM makes this system an ideal candidate for a first application of the SCOZA. Due to the fact that energy and virial route happen to yield exactly the same result for the GCM within the MSA (and possibly also for other closure relations), we proposed two ways of imposing thermodynamic consistency, i.e., via the energy and the compressibility route or the virial and the compressibility route. Introducing a state-dependent function  $K(\rho, \beta)$  in the MSA closure, we were able to derive three different approaches, namely, a PDE, an ODE, and an IDE, that enforce thermodynamic self-consistency. While both the ODE and PDE rely on the analytic solution provided by the MSA for this particular system, the IDE formulation is completely independent of this framework and can be applied for arbitrary systems and in combination with any closure relation. It remains to be verified whether the IDE approach is also applicable to systems with HC potentials.

While it was not possible to obtain results for the PDE approach, the two formulations that impose self-consistency

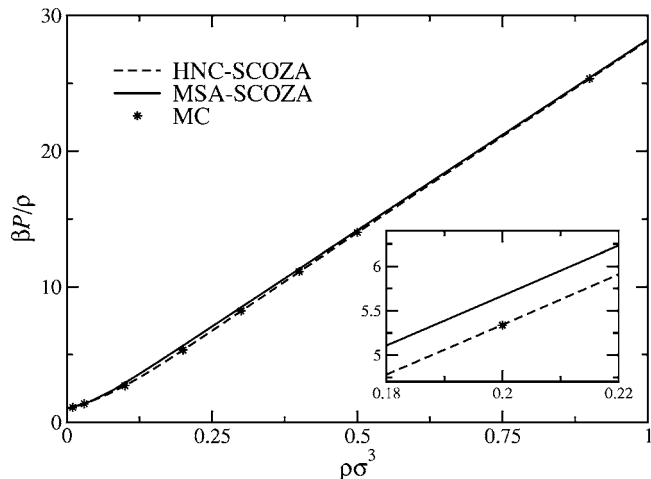


FIG. 9.  $\beta P/\rho$  as a function of  $\rho\sigma^3$  for the GCM for  $k_B T/\varepsilon=0.1$ . Note that the MSA-based SCOZA provides unphysical results for the RDF [i.e.,  $g(0)<0$ ] for  $\rho\sigma^3 \approx 1.27$ .

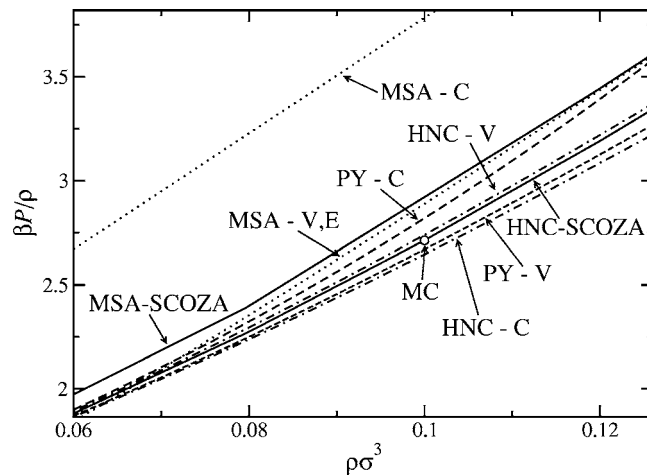


FIG. 10. Same as Fig. 9, showing an enlarged view of a limited  $\rho\sigma^3$  range. Lines and symbols as labeled.

between the virial and the compressibility route provide results for  $K(\rho, \beta)$  and  $\bar{K}(\rho, \beta)$  that are equivalent within numerical accuracy. In contrast to systems with harshly repulsive potentials the improvement of the MSA-based SCOZA approach over the MSA data is less spectacular. While it coincides with the MSA results in the limiting case of high densities where the MSA is already self-consistent, the (MSA-based) SCOZA represents a substantial improvement at small densities and low temperatures where the thermodynamic inconsistency of the MSA is more pronounced. Replacing the conventional SCOZA relation by a HNC-type closure that contains an analogous state-dependent function  $\bar{K}_{\text{HNC}}(\rho, \beta)$ , we are able to improve the HNC data for the structural as well as for the thermodynamic properties of the system. With this generalized approach we have not only demonstrated the flexibility and power of the IDE approach but have also proposed what may turn out to become a reliable liquid state theory for systems with bounded potentials.

## ACKNOWLEDGMENTS

The authors are indebted to Dieter Gottwalt (TU Wien) for numerical help, Elisabeth Schöll-Paschinger (Universität Wien) and Michael Kunzinger (Universität Wien) for useful discussions and to María-José Feraud for critical reading of the manuscript. This work was supported by the Österreichische Forschungsfonds (FWF) under Project Nos. P15758 and P17823 and by the Gemeinde Wien under Project No. H-1080/2002. One of the authors (B.M.M.) gratefully acknowledges financial support of the Erwin Schrödinger Institute for Mathematical Physics (Wien), where part of this work was carried out.

## APPENDIX: THE POLYLOGARITHM

The polylogarithm of order  $n$ ,  $\text{Li}_n(z)$ , also known as Jonquière's function,<sup>23</sup> is a complex-valued function of complex argument  $z$ , defined by

$$\text{Li}_n(z) = \frac{z}{\Gamma(n)} \int_0^\infty dt \frac{t^{n-1}}{e^t - z}, \quad (\text{A1})$$

where  $n$  is a positive, real parameter. If  $z \in \mathbb{R} \setminus (1, \infty)$ , then the polylogarithm is real valued.<sup>24</sup> For  $|z| < 1$  the polylogarithm can be evaluated as a power series,

$$\text{Li}_n(z) = \sum_{k=1}^{\infty} \frac{z^k}{k^n}. \quad (\text{A2})$$

A relation that turned out to be useful for the present application is

$$\frac{d}{dz} \text{Li}_n(z) = \frac{1}{z} \text{Li}_{n-1}(z). \quad (\text{A3})$$

A detailed list of additional, helpful relations for this function can be found in Ref. 25.

The polylogarithm was introduced in Ref. 14 to calculate the thermodynamic properties of the GCM within the MSA where, obviously, expression (A2) was used throughout; this was done even though there was no guarantee that for certain state points the modulus of the respective arguments  $|z|$  does not exceed 1, violating thus the condition for the validity of Eq. (A2). Since this function plays a central role in the formalism of the MSA and the SCOZA (see Secs. II and III), a reliable evaluation of  $\text{Li}_n(z)$  for arbitrary argument  $z$  is indispensable for a successful solution of the SCOZA-ODE and PDE. We therefore provide in the following a more detailed presentation of evaluation schemes and indicate how this function can be calculated in an accurate and efficient way for arbitrary argument  $z$ .

In its evaluation of  $\text{Li}_n(z)$ , the MATHEMATICA software relies on Euler-MacLaurin summation, expansions in terms of incomplete Gamma functions, and numerical quadrature.<sup>22</sup> Efficient and accurate C- or FORTRAN-based implementations, on the other hand, are more difficult to find. First attempts to evaluate Eq. (A1) directly by various numerical integration schemes turned out to be either too time consuming or did not provide results of sufficient accuracy. Finally, we found that the following functional relation between the polylogarithm and the complete Fermi-Dirac function,  $F_n(z)$ ,

$$F_n(z) = \frac{1}{\Gamma(n+1)} \int_0^\infty dt \frac{t^n}{e^{t-z} + 1} = -\text{Li}_{n+1}(-e^z), \quad (\text{A4})$$

along with the accurate and efficient implementation of  $F_n(z)$  via series and asymptotic expansions in combination with

Chebyshev fits, as implemented in the GNU Scientific Library,<sup>26</sup> provided the desired results, which finally brought the solution of the SCOZA differential equations within reach.

<sup>1</sup>J.-P. Hansen and I. R. McDonald, *Theory of Simple Liquids*, 2nd ed. (Academic, New York, 1986).

<sup>2</sup>C. Caccamo, Phys. Rep. **274**, 1 (1996).

<sup>3</sup>F. J. Rogers and D. A. Young, Phys. Rev. A **30**, 999 (1984).

<sup>4</sup>Y. Rosenfeld and N. W. Ashcroft, Phys. Rev. A **20**, 1208 (1979).

<sup>5</sup>J.-P. Hansen and G. Zerah, Phys. Lett. **108**, 277 (1985); G. Zerah and J.-P. Hansen, J. Chem. Phys. **84**, 2336 (1986).

<sup>6</sup>J. S. Høye and G. Stell, J. Chem. Phys. **67**, 439 (1977); Mol. Phys. **52**, 1071 (1984).

<sup>7</sup>A. Parola and L. Reatto, Adv. Phys. **44**, 211 (1995); A. Reiner and G. Kahl, Phys. Rev. E **65**, 046701 (2002); J. Chem. Phys. **117**, 4925 (2002).

<sup>8</sup>C. N. Likos, Phys. Rep. **348**, 267 (2001).

<sup>9</sup>A. Lang, C. N. Likos, M. Watzlawek, and H. Löwen, J. Phys.: Condens. Matter **12**, 5087 (2000).

<sup>10</sup>M.-J. Feraud, E. Lomba, and L. L. Lee, J. Chem. Phys. **112**, 810 (2000).

<sup>11</sup>E. Schöll-Paschinger, J. Chem. Phys. **120**, 11698 (2004).

<sup>12</sup>L. Blum and J. S. Høye, J. Stat. Phys. **19**, 317 (1978); E. Arrieta, C. Jedrzejek, and K. N. Marsh, J. Chem. Phys. **95**, 6806 (1991).

<sup>13</sup>F. H. Stillinger, J. Chem. Phys. **65**, 3968 (1976).

<sup>14</sup>A. A. Louis, P. G. Bolhuis, and J.-P. Hansen, Phys. Rev. E **62**, 7961 (2000).

<sup>15</sup>A. A. Louis, P. G. Bolhuis, J.-P. Hansen, and E. J. Meijer, Phys. Rev. Lett. **85**, 2522 (2000).

<sup>16</sup>I. O. Götzke, H. M. Harreis, and C. N. Likos, J. Chem. Phys. **120**, 7761 (2004).

<sup>17</sup>D. Pini, G. Stell, and N. B. Wilding, Mol. Phys. **95**, 483 (1998).

<sup>18</sup>E. Schöll-Paschinger, *Phase Behaviour of Simple Fluids and Their Mixtures*, Ph.D. thesis, Technische Universität Wien, 2002.

<sup>19</sup>C. Caccamo, G. Pelicane, D. Costa, D. Pini, and G. Stell, Phys. Rev. E **60**, 5533 (1999).

<sup>20</sup>Note, that the "correct" diffusion equation for nonconstant diffusivity  $D(\varrho, \beta)$  would read

$$\frac{\partial u}{\partial \beta} = \frac{\partial}{\partial \varrho} \left( D(\varrho, \beta) \frac{\partial u}{\partial \varrho} \right).$$

<sup>21</sup>W. H. Press, S. A. Teukolsky, W. T. Vetterling, and B. P. Flannery, *Numerical Recipes in FORTRAN: The Art of Scientific Computing*, 2nd ed. (Cambridge University Press, Cambridge, 1992).

<sup>22</sup>S. Wolfram, *The Mathematica Book*, 5th ed. (Wolfram Media, Champaign, 2003).

<sup>23</sup>Wolfram Research: mathworld.wolfram.com/Polylogarithm.html.

<sup>24</sup>D. Wood, University of Kent, Computing Laboratory, Report No. 15-92, 1992 (unpublished).

<sup>25</sup>Wolfram Research: functions.wolfram.com/ZetaFunctionsandPolylogarithms/PolyLog/.

<sup>26</sup>M. Galassi et al., *GNU Scientific Library Reference Manual*, 2nd ed. (Network Theory Limited, Bristol, 2005); see also www.gnu.org/software/gsl.